

# Optimum Design of the Outer Rotor Brushless DC Permanent Magnet Motor with Minimum Torque Ripples

V. Naeini\* and N. Sadeghi

Department of Electrical Engineering, Malayer University, Malayer, Iran.

**Abstract**— This research paper focuses on the optimal configuration of an outer rotor permanent magnet brushless DC (ORBLDC) motor. As torque ripple is a drawback associated with this type of motor, the study proposes an optimal design to minimize torque fluctuations. The proposed design approach considers factors such as slot width, pole arc (pole span), the number of slots, and the least common multiple factors between the number of poles and slots. Initially, the machine's parameters and dimensions are determined using design equations, and then different configurations are evaluated using the finite element method to achieve reduced torque fluctuations. The findings demonstrate that the combined design methods employed effectively minimize output torque ripples. Considering various design factors and employing advanced optimal techniques can contribute to the development of more efficient and reliable motor designs as well as reducing torque ripples.

**Keywords**—Outer rotor permanent magnet brush less DC motor, torque ripple, finite element method (FEM).

## 1. INTRODUCTION

Currently, permanent magnet brush-less DC motors (BLDC) have received considerable attention in many literatures and become the hotspot of researches. These motors have gained popularity due to their superior power density, efficiency and unique features when compared to other electric motors. They find extensive applications in various fields such as aeronautics, robotics, instrumentation, conveyor belts, and air conditioning systems [1, 2]. These motors are a type of permanent magnet synchronous motors or a conventional DC motors that use Hall effect sensors to detect the rotor position and control the current in the stator windings. Structurally BLDC motors can be categorized into two types: inner rotor and outer rotor. In inner rotor motors, the permanent magnet poles rotate inside the motor while the stator remains stationary on the outside. In contrast, in outer rotor motors, the outer part of the motor rotates, and the permanent magnet poles move within the rotor core while the stator windings remain fixed on the inside. Outer rotor brushless motors are advantageous in low-speed applications as they can have a high number of poles, eliminating the need for a mechanical gearbox. This design offers benefits such as higher torque, increased efficiency, reduced weight, and cost-effectiveness [3]. In addition, the exterior-rotor PMSG for direct-drive wind turbine applications are suitable for wind power applications because of their high efficiency and torque density [4]. While permanent magnet BLDC motors offer satisfactory performance and advantages in many applications, there is still room for improvement in certain performance characteristics. One notable drawback is torque ripples, which can lead to motor vibration and noise. These ripples occur due to the interaction between the rotor's permanent magnet poles and the stator teeth, resulting in

energy variations in the air gap as the rotor angle changes [5]. There is a relationship between the torque ripple and the magnetic energy that is stored in the magnetic field along the air gap of the PM machine. Thus a variation in the magnetic energy is leded the fluctuation in torque [6].

In recent years, various design methods have been introduced to reduce torque fluctuations, which can be broadly categorized into two groups: optimization in machine excitation control and optimization in machine structure. In first group, torque ripple reduction is achieved by optimal shaping of the stator current waveform [7–11]. The major disadvantage of this method is relatively higher complexity introduced by the power electronic converter used to control the drive circuitry. But, second group can be classified according to which part of the machine structure was modified to reduce the torque ripples. However, the majority of these methods focus on optimizing the geometric structure of the rotor or stator [12]. Some of these techniques include skewing the stator or rotor core to improve the torque ripples [13, 14]. It is shown that skewing the stator slot opening distributes the effects of the interaction between the PM edge and the stator teeth during rotation of rotor. In [15] Based on incorporating artificial slots on the stator teeth, the optimization process aims to propose an optimal machine geometry to improve torque ripple and average torque. Another of these techniques, consider slot dimensions on the low-order electromagnetic force of the machine was analyzed individually. Afterwards, a comprehensive analysis was conducted to select the optimal parameters for optimizing the stator slot structure [16, 17]. Utilizing A new segmented permanent magnet poles was proposed to modify the magnetic energy variation and the torque fluctuation [18, 19]. Other studies have proposed optimizing the shape and magnetization direction of the permanent magnet poles in different orientations to minimize induced back EMF and torque fluctuations [20, 21]. However, the electromagnetic excitation caused by variations in the torque fluctuation as a result of the magnetization distribution of the PM according to rotor position generates vibration and noise, which is a major problem. In addition to the aforementioned techniques, researchers have utilized optimization algorithms like genetic algorithms to obtain the optimal configuration for minimizing torque ripples. However, when evaluating these structures, multiple

Received: 20 Dec. 2023

Revised: 22 Jan. 2024

Accepted: 23 Jan. 2024

\*Corresponding author:

E-mail: vnaeini@malayeru.ac.ir (V. Naeini)

DOI: 10.22098/joape.2024.14250.2093

Research Paper

© 2024 University of Mohaghegh Ardabili. All rights reserved

performance measures need to be considered, leading to multi-objective optimization problems. By introducing weighting factors, such problems can be considered as single-objective problems and traditional optimization methods can be applied [22, 23].

Given these contexts, and the constant need for improving electrical machines in general, the objective of this paper is to analyze the design and improve the performance of an outer rotor BLDC motor, aiming to achieve maximum output torque and efficiency while minimizing torque ripples. To accomplish this, several efficient methods in motor design are compared and combined. A 1500-watt, 3-phase, 16-pole OR-BLDC motor is specifically designed for this study. Initially, the parameters and dimensions of the motor are determined using the genetic algorithm and sizing equations to maximize output torque density and efficiency. Subsequently, important techniques for minimizing torque ripples, such as evaluating the impact of slot number, fractional slot pitch, slot opening width, and pole span, are assessed using the finite element method (FEM).

## 2. THE INITIAL DESIGN ALGORITHM OF OR-BLDC MOTOR

Designing an electric machine requires a comprehensive understanding of various fields such as magnetics, mechanics, thermodynamics, electronics, acoustics, and materials science. Additionally, knowledge about the operating conditions of electrical machines is crucial. Therefore, with sufficient information about electric machines, an optimal design of the desired objective function, can be obtained. Based on this, the objective of this paper is to design a permanent magnet OR-BLDC motor, with maximizing torque density and efficiency while minimizing torque ripple. However, as the objective function becomes more complex, finding the desired solution becomes more challenging. Therefore, the initial objective function focuses on maximizing torque density and efficiency, and then various methods are implemented to reduce torque ripple in the motor structure.

The three-dimensional schematic of the motor under study is depicted in Fig. 1. The parameters and dimensional values of the permanent magnet OR-BLDC motor are determined as follows. In ideal conditions, the induced voltage in each phase armature winding and the generated electromagnetic torque can be calculated using the following equations [24]:

$$|E_e| = 2PZ_{slot}B_gL_sR_{so}\omega_m = K_e\omega_m, \quad (1)$$

$$\frac{|T_e|}{2PZ_{slot}B_gL_sR_{so}I_{ph}} = \frac{E_e i}{\omega_m I_{ph}} = K_t I_{ph}. \quad (2)$$

where,  $P$  represents the number of poles,  $Z_{slot}$  represents the number of conductors per slot,  $L_s$  is the length of the machine,  $R_{so}$  is the outer radius of the stator, and  $I_{rms}$  is the phase effective current. Additionally,  $K_e$  and  $K_t$  are the back-emf and torque coefficients, respectively, which are equal in this particular machine.

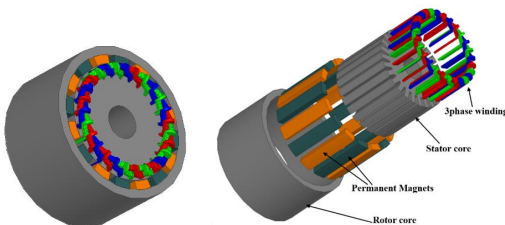


Fig. 1. The detailed 3-dimensional schematic of the OR-BLDC motor.

To calculate the magnetic flux density and magnetic flux leakage in different parts of the core, it is necessary to identify the paths of these fluxes in the magnetic structure of the machine. The approximate magnetic equivalent circuit of the motor under study, with a pair of poles, is shown in Fig. 2. By analyzing this circuit, the relationship between the fluxes passing through the air gap and different sections of the core can be determined. For this purpose, the air gap flux ( $\varphi_g$ ) and air gap flux density ( $B_g$ ) can be calculated based on the flux ( $\varphi_r$ ), and flux density ( $B_r$ ) of the permanent magnet poles, as follows.

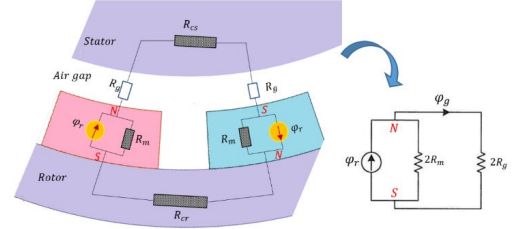


Fig. 2. The magnetic equivalent circuit between adjacent two poles of OR-BLDC motor.

Considering the magnetic equivalent circuit in Fig. 2 and for the sake of simplicity, assuming ideal rotor and stator cores, the magnetic flux per poles in the air gap can be calculated as:

$$\varphi_g = \frac{R_m}{(R_g + R_m)} \varphi_r. \quad (3)$$

where  $R_m$  and  $R_g$  represent the reluctance of the permanent magnet pole and the air gap sections, respectively. Based on the relationships of these reluctances, the relationship between the air gap flux density  $B_g$  and the permanent magnet pole flux density  $B_r$  can be obtained as:

$$B_g = \frac{C_\varphi l_m}{(C_\varphi l_g + l_m)} B_r. \quad (4)$$

where  $l_m$  and  $l_g$  represent the length of the permanent magnet poles and the length of the air gap, and the coefficient  $C_\varphi$  is calculated as:

$$C_\varphi = \frac{A_m}{A_g}. \quad (5)$$

where  $A_m$  and  $A_g$  represent the cross-sectional area of the permanent magnet pole and the cross-sectional area of the air gap in their reluctances relationships, respectively. Furthermore, to calculate the phases currents, the total specific electric loading factor,  $A$ , must be defined. This parameter is equal to the sum of the electric loading of the rotor and stator, and it can be calculated as follows:

$$A = A_s + A_r = \frac{N_s Z_{slot} I_{ph}}{2\pi R_{so}} + 0 = \frac{3 N_{ph} I_{ph}}{\pi R_{so}}. \quad (6)$$

where  $A_s$  represents the electric loading of the stator, which is equal to the ratio of the total ampere-turns of stator windings to the average air gap circumference, and  $A_r$  represents the electric loading of the rotor, which is zero due to the absence of excitation in the rotor. Additionally,  $N_s$  is the number of stator slots,  $Z_{slot}$  is the number of conductors inside each slot,  $I_{ph}$  is the phase current of the winding, and  $R_{so}$  is the outer radius of the stator.

By using Eq. (6), the phase current can be obtained as follows:

$$I_{ph} = \frac{A \pi R_{so}}{3 N_{ph}}. \quad (7)$$

To determine the other design parameters of the OR-BLDC motor, considering the various objectives in different applications, it is necessary to define a suitable objective function. Since the typical goal of the outer rotor motors is to achieve high torque density and efficiency in machine performance, in this paper, the motor constant,  $K_m$ , as defined in Eq. (8), is used for this purpose. In this equation, the desired performance of the BLDC motor is emphasized by maximizing the motor constant,  $K_m$ , which corresponds to the highest torque density and efficiency.

$$K_m = \frac{|T_{den}|}{N_s R_{slot} I_{ph}^2}. \quad (8)$$

As evident in Eq. (8), the motor constant is proportional to the torque density and inversely proportional to the total copper losses which are the dominant losses in the machine. Therefore, optimizing this objective function implies maximizing the torque density while minimizing copper losses or increasing efficiency. In this case, such an objective function ensures higher torque production and lower losses. In this equation,  $N_s$  represents the total number of stator slots, and  $R_{slot}$  is the electrical resistance of the conductors in each slot, which can be derived as follows:

$$R_{slot} = \frac{\rho L_s Z_{slot}}{A_{wb}} = \frac{\rho L_s Z_{slot}^2}{K_{wb} A_s}. \quad (9)$$

Where  $\rho$  is the specific resistance of the conductor in ohms per meter,  $A_{wb}$  is the cross-sectional area of each conductor,  $K_{wb}$  is the slot fill factor, and  $A_s$  is the cross-sectional area of the slot which can be calculated as:

$$A_s = \frac{\pi}{N_s} [(R_{so} - d_1 - d_2)^2 - (R_{si} + W_{sy})^2] - W_{st}. \quad (10)$$

The dimensions of the stator slot and tooth are shown in Fig. 3.

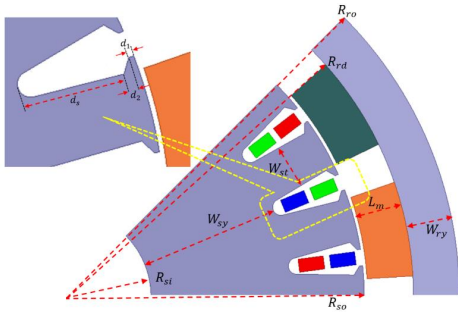


Fig. 3. The dimensions of the stator slot and tooth of OR-BLDC motor.

As shown in Fig. 3,  $W_{st}$  represents the width of the stator tooth and is derived as:

$$W_{st} = \frac{2\pi R_{so} B_g}{N_s K_{st} B_t}. \quad (11)$$

where  $B_t$  is the flux density of the stator tooth, and  $K_{st}$  is the slot fill factor. The width of the stator yoke is equal to:

$$W_{sy} = \frac{\pi R_{so} B_g}{p K_{st} B_{sy}}. \quad (12)$$

where  $B_{sy}$  is the flux density of the stator yoke and similarly, the width of the rotor yoke is given by:

$$W_{ry} = \frac{\pi R_{so} B_g}{p K_{st} B_{ry}}. \quad (13)$$

Table 1. The parameters values of initial design of OR-BLDC motor.

Parameter	Symbol	Value
Rated power	$P$	1000 W
Rated voltage	$V_s$	100 V
Number of stator slots	$N_s$	24
Pole number	$P$	16
Stator inner radiuses	$R_{si}$	40 mm
Axial length of the machine	$L_s$	65 mm
Rated speed	$n$	1500 rpm
Magnetic flux density of core	$B_c$	1.5 T
Magnetic flux density of PM	$B_r$	1.21 T
Pole arc	Pole spam	70%

where  $B_{ry}$  is the flux density of the rotor yoke. On the other hand, torque density,  $T_{den}$ , in Eq. (8) is defined as the ratio of the output torque to the volume of the machine as:

$$T_{den} = \frac{T_e}{\frac{2P Z_{slot} B_g R_{so} L_{ph}}{\pi R_{ro}^2}} = \quad (14)$$

Also, the relationship between the number of phases and the number of slot conductors in a 3-phase machine is defined as:

$$N_{ph} = \frac{N_s Z_{slot}}{6}. \quad (15)$$

Now, by substituting Eqs. (7), (14), and (15) into Eq. (8) and neglecting the end-winding resistance, the motor constant can be obtained as follows:

$$K_m = \frac{P \frac{C_{\varphi} l_m}{(C_{\varphi} l_g + l_m)} B_r K_{wb} A_s}{\pi^2 R_{ro}^2 \rho L_s A} = \frac{P \frac{C_{\varphi} l_m}{(C_{\varphi} l_g + l_m)} B_r K_{wb} \left( \frac{\pi}{N_s} [(R_{so} - d_1 - d_2)^2 - (R_{si} + W_{sy})^2] - W_{st} \right)}{\pi^2 R_{ro}^2 \rho L_s A}. \quad (16)$$

As can be seen in Eq. (16), if the coils material,  $\rho$ , and the slot fill factor,  $K_{wb}$ , are known and the value of magnetic flux density of PM pole,  $B_r$ , be constant, the motor constant of the OR-BLDC motor, depends on the parameters of electrical loading coefficient,  $A$ , the number of poles,  $P$ , the number of stator slots,  $N_s$ , the stator inner radius,  $R_{si}$ , and outer radius,  $R_{so}$ , the rotor outer radius,  $R_{ro}$ , the axial length of the machine,  $L_s$ , the air gap length,  $l_g$ , the length of the PM poles,  $l_m$ , and the dimensions of the stator slots. Therefore, all of these parameters can play a role as optimization variables to achieve maximum motor constant.

### 3. THE OPTIMUM DESIGN OF OR-BLDC MOTOR

As mentioned above, in the optimization objective function given by Eq. (16), the number of optimization variables is very high, and it is not feasible to simultaneously consider and evaluate all of them. This complexity makes the optimization problem in this objective function highly intricate and challenging. In this section, in order to simplify the optimization problem, some variables in the objective function of OR-BLDC motor are assumed to be constant. These constant parameters are chosen based on motor performance constraints and dimensional limitations, as shown in Table 1. By considering these assumptions and constraints, the optimization problem becomes more manageable and suitable for finding an appropriate solution using the genetic algorithm. Consequently, the optimization parameters of the motor constant objective function are considered as the genes of a chromosome in the genetic algorithm, considered as Table 2, according to the relationships described in previous sections.

By applying the given parameters and constraints in the genetic optimization algorithm, with the objective function being the maximum motor constant,  $K_m$ , in Eq. (16), the dimensional

Table 2. Range of changes of optimization parameters (genes of a chromosome).

Range of changes	Gene
$0.03^m \leq R_{so} \leq 0.2^m$	Stator outer radius ( $R_{so}$ )
$8000 \leq A \leq 50000$	Electrical loading coefficient (A)
$0.005^m \leq l_m \leq 0.01^m$	Length of the PM poles ( $l_m$ )
$0.004^m \leq d_s \leq 0.01^m$	Stator slot deep ( $d_s$ )
$0.0005^m \leq l_g \leq 0.001^m$	Are gap length ( $l_g$ )

Table 3. Dimensional information and other variables obtained by GA.

Parameter	Symbol	Value
Stator outer radius	$R_{so}$	150 mm
electrical loading coefficient	$A$	12000
length of the PM poles	$L_m$	9 mm
Stator slot deep	$d_s$	9.5 mm
Are gap length	$l_g$	0.54 mm

information and other variables are obtained in the initial design, as shown in Table 3.

In the following sections, the influence of other important parameters in the optimization objective function will be examined. These parameters include the number of stator slots, slot dimensions, and the angle of the permanent magnet pole arcs. The main goal is to achieve an optimal structure with the best motor performance, maximizing output torque while minimizing torque ripples. By carefully analyzing and optimizing these parameters, it will be possible to enhance the motor's efficiency, torque production, and reduce any undesirable torque ripples. Through finite element modeling of the designed machine and validation of the simulation results, the impact of these parameters will be investigated and analyzed. By studying their effects, it will be possible to determine their significance in achieving the optimal design. The investigation of these influential parameters will provide valuable insights into the design optimization process, leading to the development of an appropriate structure with superior motor performance.

#### 4. MODELLING AND EVALUATING OF OR-BLDC MOTOR

In this section, finite element modeling is utilized to validate the accuracy and correctness of the design, as well as evaluate the performance results of the designed machine. Fig. 4 illustrates the magnitude and distribution of the magnetic flux density in various parts of the machine core. It also presents a portion of the plot mesh, providing a visual representation of the magnetic field within the machine. This analysis helps to understand the behavior and characteristics of the magnetic flux within the motor.

Fig. 5 displays the output torque characteristic of the motor over time. It provides information about the torque produced by the motor and how it varies during operation. From Fig. 5, it can be observed that the average torque produced by the motor is 7.5 Newton-meters. Additionally, the torque ripple, which represents the fluctuation in torque output, is found to be 36%.

These results obtained from the finite element modeling and performance evaluation provide valuable insights into the motor's behavior and performance. They help in assessing the design's effectiveness and identifying areas for improvement. Based on the simulation results, it is evident that the torque ripples of the studied motor are high. It is important to note that in a suitable design for various applications, torque ripples should be kept to a minimum and within an acceptable range. In the subsequent sections, different motor structures will be evaluated to determine the one that minimizes output torque ripples. Various scenarios will be compared and analyzed to identify the best structure that can effectively reduce torque fluctuations. By conducting these comparisons and evaluations, it will be possible to select the

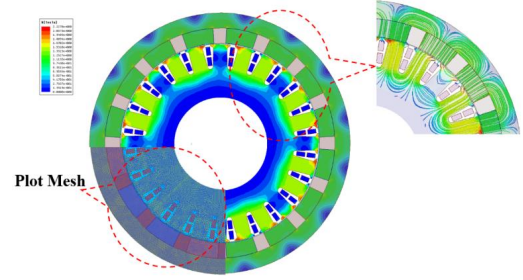


Fig. 4. Magnetic flux density in different parts of the machine core and a portion of its plot mesh.

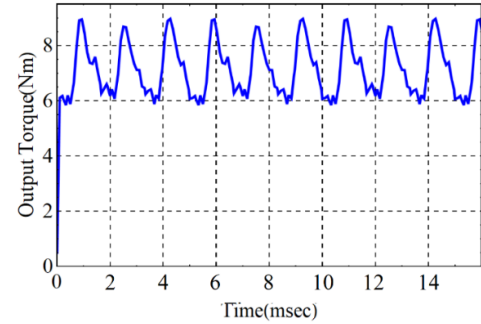


Fig. 5. The output torque characteristic of the motor over time.

optimal motor structure that provides the lowest torque ripples. This analysis is crucial in achieving a motor design that meets the performance requirements for different applications.

##### 4.1. The impact of slot number in torque ripples

In this section, the effect of changing the number of slot in the stator core on the torque ripples is evaluated. One of the most significant factors causing torque fluctuations in permanent magnet machines is the cogging torque phenomenon, which occurs due to the interaction between the permanent magnet pole fields and the non-uniformity of the stator teeth. Various investigations have shown that as the least common multiple (LCM) between the number of stator slots and the number of rotor poles decreases, the frequency of cogging torque increases and leading to a reduction in torque ripples. In fact, the components of cogging torque depend on the number of slots, poles, and their interaction with each other. Therefore, for different numbers of slots, the effects of changing the LCM between the number of stator slots and rotor poles, as well as the percentage of output torque ripples, are presented in Table 4.

As shown in the obtained results in this table, increasing the LCM reduces the torque ripple. However, in this analysis, considering the dimensions of the studied motor, the number of slots cannot exceed 45 slots. Therefore, according to the results in Table 4, the best machine structure with a stator of 45 slots and the least amount of torque ripple, i.e., 7.6%, is selected. Fig. 6 illustrates the torque characteristic of the selected structure with

Table 4. Output torque variations by changing the number of stator slots.

Case	Number of slot	LCM factor	Torque average (nm)	Torque ripples (%)
1	36.251	7.460	48	24
2	27.726	8.768	144	36
3	17.788	9.672	240	30
4	14.868	8.219	432	27
5	10.777	9.029	720	45

45 slots. This graph provides a visual representation of the motor's torque output over time.

Moving forward, this specific number of slots (45 slots) will be utilized in the examination of other influential parameters in order to further minimize torque ripples. By analyzing and optimizing these factors, it is expected to achieve a motor design with improved performance and reduced torque fluctuations.

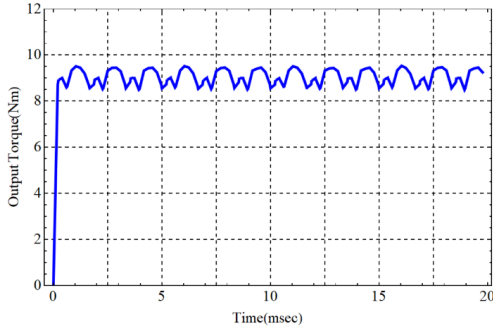


Fig. 6. Output torque of 16 poles and 45 slot OR-BLDC motor.

#### 4.2. The impact of pole arc in torque ripples

In this section, the influence of changing the distance between poles (pole span) or the ratio of pole arc to pole pitch on torque ripples is examined for the 45-slot motor from the previous section. According to Fig. 7, the magnitude of the ratio of pole arc to pole pitch in percentage, is defined by the following equation, where  $\gamma$  represents the full pole pitch and  $\beta$  is the pole arc.

$$\%Pole\ arc = \frac{\beta}{\gamma} \times 100. \quad (17)$$

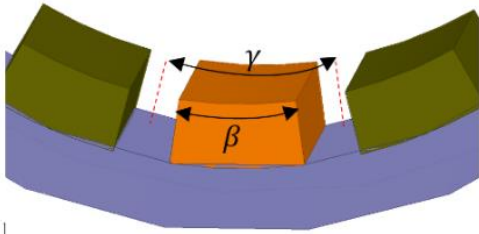


Fig. 7. Pole arc and pole pitch of OR-BLDC motor.

By varying this ratio, the impact on torque ripples can be assessed. Different values of the ratio will be investigated to determine the optimal pole span that minimizes torque fluctuations. This analysis is crucial in achieving a motor design that exhibits improved performance with reduced torque ripples. The results obtained in this section highlight that changing the distance between poles or the percentage of pole arc will result in variations in the air gap flux density. This, in turn, affects the distribution of magnetic flux between the rotor and stator cores, as well as the magnitude of leakage fluxes. The increase in leakage fluxes and the reduction in the effective value of the linkage flux between the stator and rotor cores, along with changes in the air gap flux distribution, contribute to variations in the produced torque ripple. The pole arc angle, in particular, plays a crucial role in torque ripple. In this study, different sizes of pole arc angles for a 45-slot OR-BLDC motor are evaluated. To achieve optimal motor performance, the range of pole arc angle variations is evaluated from 70% to 90% of the full pole pitch. The results of the average torque and torque ripples for different motor pole arc angles,

Table 5. Output torque variations by changing the pole span.

Case	Pole span %	Torque average (nm)	Torque ripples (%)
1	70	9.029	10.777
2	75	9.146	9.930
3	80	9.335	8.248
4	85	9.415	7.756
5	90	9.576	7.634

are summarized in Table 5. This table provides a comprehensive overview of the performance of each pole arc angle. By analyzing the data in Table 5, it will be possible to identify the pole arc angle that yields the optimal motor performance with the least torque ripple. This analysis is vital in selecting the most suitable motor design that minimizes torque fluctuations and meets the desired performance requirements.

As observed from the obtained results, increasing the pole arc angle causes increasing the magnitude of the average torque and decreasing the magnitude of its ripples. When the pole arc is increased, a stronger magnetic field linkage is resulted between the rotor and stator core, and this situation is leading to a more suitable distribution of the flux per pole. However, it should be noted that a larger pole arc angle increases the flux leakage between the adjacent poles and makes challenges of core saturation, especially in the teeth regions. Based on this, the best pole arc angle for this machine is 90 percent, as shown in the torque characteristic in Fig. 8. As seen in this figure, the torque ripple decreases from 10.8% in the case of a 70% pole arc angle to 7.6% in the case of a 90% pole arc angle.

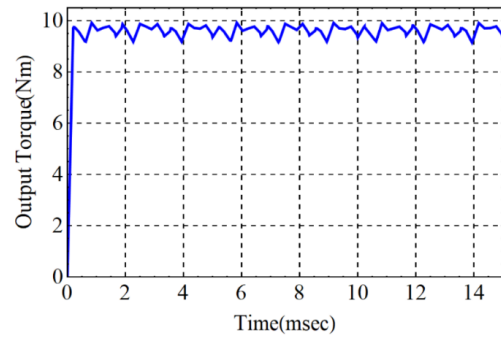


Fig. 8. Output torque of 16 poles, 45 slot and 90% pole arc OR-BLDC motor.

For preferable evaluation of results, the diagrams in Fig. 9 illustrate the effect of changing the pole arc angle and the number of stator slots on the magnitude of the output torque and its ripples. As observed in Fig. 9-(a), increasing the number of stator slots and the pole arc angle results in an increase in the magnitude of the average output torque. This is because in this case, the effective cross-section area of flux distribution in the air gap increases, and the interaction between the rotor and stator fields takes place in the best possible manner. As can be seen in Fig. 9-(b), this state also has an impact on reducing torque fluctuations, as in this increase, the magnitude of torque ripples decreases. Therefore, based on the obtained results, the number of stator slots is selected as 45 and the pole arc angle is chosen as 90 percent. An important point to note in these diagrams is that when a small pole arc angle is chosen, the distance between adjacent poles should be increased, leading to a reduction in the interaction between the rotor and stator fields and, consequently, a decrease in the produced torque. Additionally, when the pole arc angle exceeds a certain limit, it results in increased leakage flux between the poles.

In the next section, the effect of changing the dimensions of the stator slots will be evaluated in order to achieve better performance

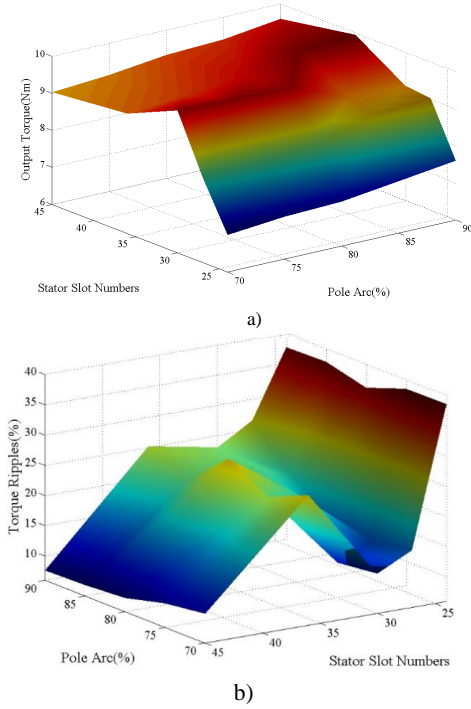


Fig. 9. a) Output torque, b) Torque ripples of OR-BLDC motor as variation of pole arc and number of stator slots.

in torque production for a 45-slot motor with a 90% pole arc. By varying the dimensions of the stator slots, such as their width, depth, or shape, it is possible to influence the distribution of the magnetic flux and the resulting torque characteristics of the motor. This analysis is crucial in optimizing the motor design to enhance its torque production capabilities.

### 4.3. The impact of the geometrical shape of stator slot in torque ripples

In this section, the effect of different dimensions of the stator slot structure on torque fluctuations, specifically cogging torque, is evaluated. The interaction between the permanent magnet poles and the geometrical shape of the stator slot is a significant factor contributing to torque fluctuations in permanent magnet machines. The results obtained from this analysis will provide valuable insights into the impact of stator slot dimensions on motor performance, enabling the selection of optimal slot dimensions for achieving superior torque production characteristics. So in this section, different dimensions of the stator slot structure are evaluated by changing the slot width parameters as shown in Fig. 10. A summary of the results of these different structures with changes in the slot width is presented in Table 6. As observed in this table, different slot structures have a considerable effect on the tooth torque magnitude and overall torque fluctuations. Generally, the cogging torque magnitude decreases when the slot opening decreases, with the best condition in this study being the last row of Table 6, which ultimately reduces torque ripples by 4.3%. Fig. 11 is provided a visual representation of the torque characteristic in this optimal slot structure.

This analysis demonstrates the importance of stator slot dimensions in minimizing torque fluctuations and enhancing the overall performance of the machine. By selecting the appropriate slot width parameters, it is possible to reduce cogging torque and achieve smoother torque output, leading to improved motor performance.

Therefore, based on the investigations conducted in the previous sections, the optimal structure for the outer rotor permanent magnet

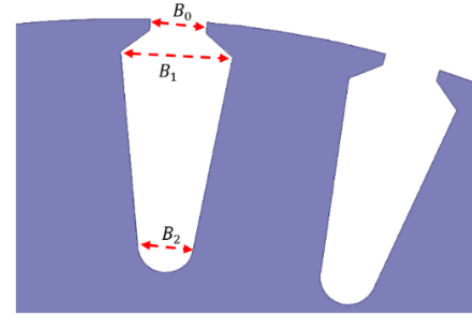


Fig. 10. The stator slot structure of OR-BLDC motor.

Table 6. Output torque variations of 16 poles, 45 slot and 90% pole arc OR-BLDC motor by changing the slot shape.

Case	$B_0$ (mm)	$B_1$ (mm)	$B_2$ (mm)	Torque average (nm)	Torque ripples (%)
1	2.5	5	2.5	9.576	7.634
2	2	4	2.5	11.562	5.615
3	1	4.5	3	9.682	5.129
4	1	4	3	10.542	4.900
5	1.5	4	3	10.678	4.531
6	2	4	3	10.779	4.343

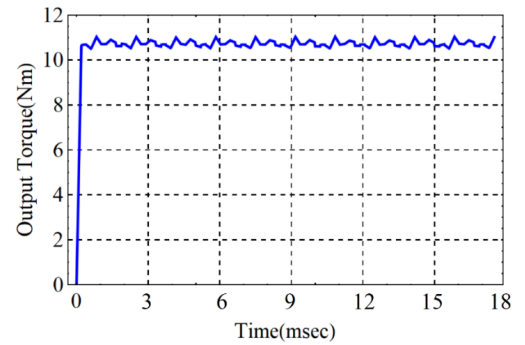


Fig. 11. Output torque of 16 poles, 45 slot and 90% pole arc OR-BLDC motor with the best slot structure.

machine is determined as follows:

- Number of poles: 16
- Number of slots in the stator: 45
- Pole arc angle: 90%
- Slot width parameters: Corresponding to the last row of Table 6, which minimizes torque fluctuations.

By selecting this specific configuration and optimizing the slot width parameters, the torque ripple is significantly reduced from the initial value of 36% to just 4%. This selection ensures that the machine operates with improved torque production capabilities, reduced torque fluctuations, and enhanced overall performance. These findings highlight the importance of thorough analysis and optimization of various design parameters in order to achieve the desired performance characteristics in a permanent magnet machine.

## 5. CONCLUSION

This paper focused on the design and optimization of an outer rotor permanent magnet brushless DC motor (OR-BLDC). First, the design equations of the OR-BLDC were presented, providing a foundation for the subsequent optimization process. Then, a genetic algorithm approach was employed to achieve an initial optimal design with maximum efficiency and torque density. By considering initial information and constraints, the algorithm aimed to find the best motor constant. Furthermore, the impact of the

number of stator slots, slot dimensions, and pole arc angle on motor performance was thoroughly examined. The goal was to achieve a suitable motor structure with the best performance, specifically maximum torque with minimal torque ripple. Finally, a combined approach utilizing the finite element method was used to reduce torque ripple. By employing this method, the torque ripple was successfully reduced to 4%.

Overall, this study demonstrated the importance of design optimization and parameter analysis in achieving improved performance in OR-BLDC machines. By considering various design factors and employing advanced techniques, such as genetic algorithms and finite element analysis, it is possible to enhance motor efficiency, torque density, and reduce torque ripple. These findings can contribute to the development of more efficient and reliable motor designs in various applications.

## REFERENCES

- [1] J. F. Gieras, *Permanent magnet motor technology: design and applications*. CRC press, 2009.
- [2] Y. Song, G. Liu, S. Yu, H. Wang, and F. Zhang, "Investigation of a low-speed high-torque-density direct-drive external-rotor pmsm for belt conveyor application," *IEEE Access*, 2023.
- [3] T.-Y. Lee, M.-K. Seo, Y.-J. Kim, and S.-Y. Jung, "Motor design and characteristics comparison of outer-rotor-type bldc motor and blac motor based on numerical analysis," *IEEE Trans. Appl. Supercond.*, vol. 26, no. 4, pp. 1–6, 2016.
- [4] A. Abdoos, M. Moazzen, and S. Hosseini, "Optimal design of an exterior-rotor permanent magnet generator for wind power applications," *J. Oper. Autom. Power Eng.*, vol. 9, no. 3, pp. 193–202, 2021.
- [5] M. Amirkhani, M. A. Ghanbari, M. A. J. Kondelaji, M. Mirsalim, and A. Khorsandi, "Performance analysis of outer rotor multi-tooth biased flux permanent magnet motors," *IEEE Trans. Energy Convers.*, 2023.
- [6] Y. ÖZOĞLU, "New magnet shape for reducing torque ripple in an outer-rotor permanent-magnet machine," *Turk. J. Electr. Eng. Comput. Sci.*, vol. 25, no. 5, pp. 4381–4397, 2017.
- [7] H. Masoudi, A. Kiyoumars, S. M. Madani, and M. Ataei, "Torque ripple reduction of non-sinusoidal brushless dc motor based on super-twisting sliding mode direct power control," *IEEE Trans. Transp. Electrification*, 2023.
- [8] S. Hajiaghahi, Z. Rafiee, A. Salemmia, and M. Aghamohammadi, "Optimal sensorless four switch direct power control of bldc motor," *J. Oper. Autom. Power Eng.*, vol. 7, no. 1, pp. 78–89, 2019.
- [9] A. Dejamkhooy and A. Ahmadpour, "Torque ripple reduction of the position sensor-less switched reluctance motors applied in the electrical vehicles," *J. Oper. Autom. Power Eng.*, vol. 11, no. 4, pp. 258–267, 2023.
- [10] D. Liao, L. Yu, and Z. Liu, "A torque ripple reduction method using field current injection for doubly salient motor," *Energy Rep.*, vol. 8, pp. 573–581, 2022.
- [11] S. K. Neogi and K. Chatterjee, "A modified brush-less dc motor having high torque density and its simplified current control technique," *IEEE Trans. Ind. Electron.*, 2022.
- [12] H. Sun, G. Krebs, I. Bahri, P. Rodriguez-Ayerbe, and M. Khanchoul, "Pmsm design optimization concerning sensorless performance and torque ripple," *E-Prime-Adv. Electr. Eng. Electron. Energy*, vol. 2, p. 100049, 2022.
- [13] I.-H. Jo, J. Lee, H.-W. Lee, J.-B. Lee, J.-H. Lim, S.-H. Kim, and C.-B. Park, "Analysis of optimal rotors skew to improve the total harmonic distortion of back electromotive force in mg-pmsm for traction," *IEEE Access*, vol. 11, pp. 122231–122237, 2023.
- [14] C.-M. Lee, H.-S. Seol, J.-y. Lee, S.-H. Lee, and D.-W. Kang, "Optimization of vibration and noise characteristics of skewed permanent brushless direct current motor," *IEEE Trans. Magn.*, vol. 53, no. 11, pp. 1–5, 2017.
- [15] E. Brescia, M. Palmieri, P. R. Massenio, G. L. Cascella, and F. Cupertino, "Cogging torque suppression of modular permanent magnet machines using a semi-analytical approach and artificial intelligence," *IEEE Access*, 2023.
- [16] J. Chen and S. Ding, "Investigation on the influence of slot dimensions of spmsm on electromagnetic force," in *2023 26th Int. Conf. Electr. Mach. Syst. (ICEMS)*, pp. 1561–1565, IEEE, 2023.
- [17] O. Tosun and N. Serteller, "Analysis of brushless direct current motor stator slot geometry and winding type with fem," in *Proc. 3rd Int. Symp. Multidiscip. Stud. Innovative Technol. (ISMSIT), Ankara, Turkey*, pp. 20–22, 2019.
- [18] M. Toren, "Determination of the performance parameters of a gearless direct-drive inner-rotor pmbldc motor via different slot–magnet combinations," *Iran. J. Sci. Technol. Trans. Electr. Eng.*, vol. 48, no. 1, pp. 127–142, 2024.
- [19] Z. Xing, W. Zhao, X. Wang, and Y. Sun, "Reduction of radial electromagnetic force waves based on pm segmentation in spmsms," *IEEE Trans. Magn.*, vol. 56, no. 2, pp. 1–7, 2020.
- [20] T. Jhankal and A. N. Patel, "Design and cogging torque reduction of radial flux brushless dc motors with varied permanent magnet pole shapes for electric vehicle application," *Trans. Energy Syst. Eng. Appl.*, vol. 4, no. 2, pp. 1–13, 2023.
- [21] Z. S. Du and T. A. Lipo, "High torque density and low torque ripple shaped-magnet machines using sinusoidal plus third harmonic shaped magnets," *IEEE Trans. Ind. Appl.*, vol. 55, no. 3, pp. 2601–2610, 2019.
- [22] S. B. Bae, D. S. Choi, and S. G. Min, "Artificial hunting optimization: A novel method for design optimization of permanent magnet machines," *IEEE Trans. Transp. Electrification*, 2023.
- [23] G. Bramerdorfer, "Multiobjective electric machine optimization for highest reliability demands," *CES Trans. Electr. Mach. Syst.*, vol. 4, no. 2, pp. 71–78, 2020.
- [24] D. C. Hanselman, *Brushless permanent magnet motor design*. The Writers' Collective, 2003.